NASA Technical Memorandum 73291

Altimeter Rain Detection

E. J. Walsh

July 1981

NASA
National Aeronautics and Space Administration

Wallops Flight Center
Wallops Island, Virginia 23337
AC 804 824-3411

NASA Technical Memorandum 73291

Altimeter Rain Detection

E. J. Walsh

NASA Wallops Flight Center
Wallops Island, Virginia 23337

National Aeronautics and
Space Administration

Wallops Flight Center
Wallops Island, Virginia 23337
AC 804 824-3411

ALTIMETER RAIN DETECTION

Edward J. Walsh
NASA Wallops Flight Center
Wallops Island, VA 23337

ABSTRACT

The purpose of this paper is to outline a proposed implementation of a rain detection capability for the NOSS radar altimeter which would require only minor hardware modifications to the basic SEASAT altimeter design (MacArthur, 1978) and indicate the expected level of performance.

GEOPHYSICAL MODEL OF RAIN

In estimating rain rate using short pulse radar techniques from a beam-limited satellite-borne radar altimeter, we are concerned with the reflectivity or radar cross section of rain at different altitudes above the surface tracked. Figure 1 shows the measured reflectivity versus altitude for various rain rates. The reflectivity is approximately constant with altitude over the vertical extent of the rain which is typically concentrated in the range 3.5 to 5 km above the surface. Figure 2 shows what the reflectivities of Figure 1 would translate into as far as power received at the NOSS altimeter, assuming that the vertical extent of the rain is 5 km. There are four curves indicated on the figure for ranges corresponding to just above the surface, and 1 km, 3 km, and 5 km above the surface. The greatest received power would be from the top of the rain. At lower altitudes, the effective received backscatter is less due to absorption by the rain above. (The information in Figures 1, 2 and 4 was extracted from Figures 9, 6 and 8, respectively of Goldhirsh and Rowland (1980).)

For soundings by a short pulse radar such as the NOSS altimeter, the backscatter return may be modeled as a Rayleigh process in which the received pulse power is an exponentially distributed random variable with a standard deviation equal to the mean. Not indicated in Figure 1 is the effect of the bright band, which is the region at the top of the rain and near the freezing temperature of water. In the bright band, ice crystals become coated with a layer of water and produce anomalously large reflections.

There is generally a bright band associated with the top of any rain system, and the NOSS altimeter implementation for rain detection would have to employ range gating to exclude the bright band to ensure valid results.

PROPOSED RAIN DETECTION IMPLEMENTATION FOR THE NOSS ALTIMETER

In normal surface tracking, the NOSS altimeter operates in a closed-loop tracking mode on 926 per second chirped pulses and outputs smoothed range and surface waveform data every 50 ms. For altimeter rain detection, it is proposed that one 50 ms interval per second be allocated to measurement of rain backscatter using CW pulses. Thus, once per second, for a period of 0.05 second, the altimeter would operate in a CW rain detection mode. This mode would be very similar to the altimeter acquisition mode in which unmodulated CW pulses are transmitted. During the 50 ms rain detection period, no altimeter range data would be obtained and the closed-loop range tracker would coast.

The normal altimeter acquisition mode finds the time of arrival of the maximum CW return signal and determines its range. For rain detection, modifications must be made to permit CW received signal power measurements at fixed altitudes above the surface tracked by the altimeter tracking loop.

The recommended technique is to determine the returned power at two fixed offsets from the ocean surface, 1 km and 3 km. The hardware modifications to the altimeter acquisitions circuitry would be simple, requiring an additional comparator to provide an enabling signal to the detector output when the desired range was reached (Figure 3). The predetection filter would also be narrowed to match it to the CW pulse bandwidth and reduce the noise power. Alternatively, parallel signal processing circuitry for rain detection could be added to the SEASAT acquisition circuitry, with bandwidths and time constants optimized for rain backscatter measurements.

ADVANTAGES OF TWO ALTITUDE MEASUREMENTS

Examining rain backscatter at two altitudes and generating averages and differences of the two values would provide a great deal of flexibility without reducing accuracy. For low rain rates, where Figure 2 shows little difference between the curves, the averaged value would provide the same information at the same accuracy as if only one range had been interrogated in the 50 ms period.

At the higher rain rates, the difference value would provide a rain rate measure that could be more accurate than that obtained from a single altitude if the rain storm did not fill the antenna beam. Figure 4 indicates the typical diameters of rain storms as a function of rain rate. For the higher rates, it is apparent that the storms will not generally fill the beam. If the beam were only half filled, the power returned from each of the two altitudes measured would drop by a factor of 2 or 3 dB. If only one altitude had been interrogated, one could not differentiate between a heavy rain filling a portion of the beam or a light rain filling the beam. However, the interrogation of two altitudes provides two different measures whose difference can be used to estimate the true rain rate (the difference of the two measures is not affected by a storm not filling the beam because the backscattered power at both ranges is reduced by the same amount). The reduction of the power values below those indicated in Figure 2 would provide a measure of the beam filled by the rain storm.

ALTIMETER TIMING FOR RAIN DETECTION

Figure 5 indicates the arrangement of the transmitted and received pulses in the proposed rain detection implementation. For the first 19/20 of each second, the altimeter would function in its normal manner transmitting chirp pulses. Then, during the last 1/20 of each second, the transmitter would switch to the CW transmit mode and transmit a sequence of 50 pulses. The way the hardware is configured, the decision to operate with CW rather than chirp pulses is made just before transmission and impacts the ability of the altimeter received to process chirp signals still in transit. As is shown in Figure 5, the last five pulses transmitted in the chirp mode will be lost because they were still in transit when the mode switch was made. Similarly, the last five pulses transmitted in the CW mode will be lost when the transmitter is switched back to chirp.

During the CW mode, the altimeter range tracker would coast. This will result in a negligible degradation of the range and SWH data (approximately 350 m of ocean surface track would be lost every 7 km). On a one second average, the noise in the range and SWH measurements would increase by about 2.5 percent; this is considered to be an acceptable penalty.

RAIN DETECTION MEASUREMENT PERFORMANCE

We now consider the rain backscatter measurement performance achievable with the proposed NOSS altimeter implementation. A total of 45 pulses (CW) are available in the 50 ms rain detection interval. It is proposed that 20 pulses be used to measure rain rate at each of two altitudes above the surface. This leaves five pulses to determine the range to the top of the bright band for a measure of the rain thickness (Figure 6). The plot in Figure 7 shows the results of a simulation of how the altimeter AGC would settle over a series of 45 pulses starting with an initial value of 7 dB above the receiver system noise. The jagged curve represents the detected power fluctuations if there were only receiver noise present. At each step, if the power exceeds the threshold level established by the AGC value, the AGC is incremented 1 dB. A better starting point for the range of power expected (0 to 15 dB above receiver noise) would appear to be 8 dB with the AGC increments indicated at the top of Figure 7. The signal plus noise power an exponentially distributed random variable. Since the AGC will settle out at the median value, it will be offset below the true mean value of received power by 1.6 dB (Figure 8).

Figure 9 indicates for the average of 100 trials, the manner in which the altimeter AGC approaches the mean value for values of signal plus noise of -110, -105, -100, and -95 dBm. The dashed curves indicate the mean AGC behavior for an 80 kHz post-detection filter (Figure 3) which would average over two range cells vertically. The standard deviation is reduced and so is the offset because the power would no longer be exponentially distributed. The average standard deviation for integrating the power over two range cells is 1.13 dB.

Figure 10 shows simulation results for one altimeter pass where rains of various rates were overflown where the encountered periods were determined by the average storm diameters of Figure 4. Figure 11 shows the same data after a two-point along-track data averaging. The bottom curve represents the mean backscattered power level for the two altitudes. The mean power diminished at 25 and 30 mm/hr because the antenna beam was not filled. The top curve is the difference of the backscattered power at the two altitudes and is correspondingly more noisy. However, the encounter period from the bottom curve could be used to determine the averaging time for the top curve to reduce the noise level. While detailed data processing algorithms need to be developed, the simulation signatures appear to have substantial promise for providing operation estimates of average rain rate.

REFERENCES

Goldhirsh, J. and J. R. Rowland (1980), "Assessment of Atmospheric Heights Uncertainties for High Precision Satellite Altimeter Missions to Monitor Ocean Currents," Johns Hopkins University/Applied Physics Laboratory Report S1R80U-018, June.

MacArthur, J. L. (1978), "SEASAT-A Radar Altimeter Design Description," Johns Hopkins University/Applied Physics Laboratory Report SDO-5232, November.

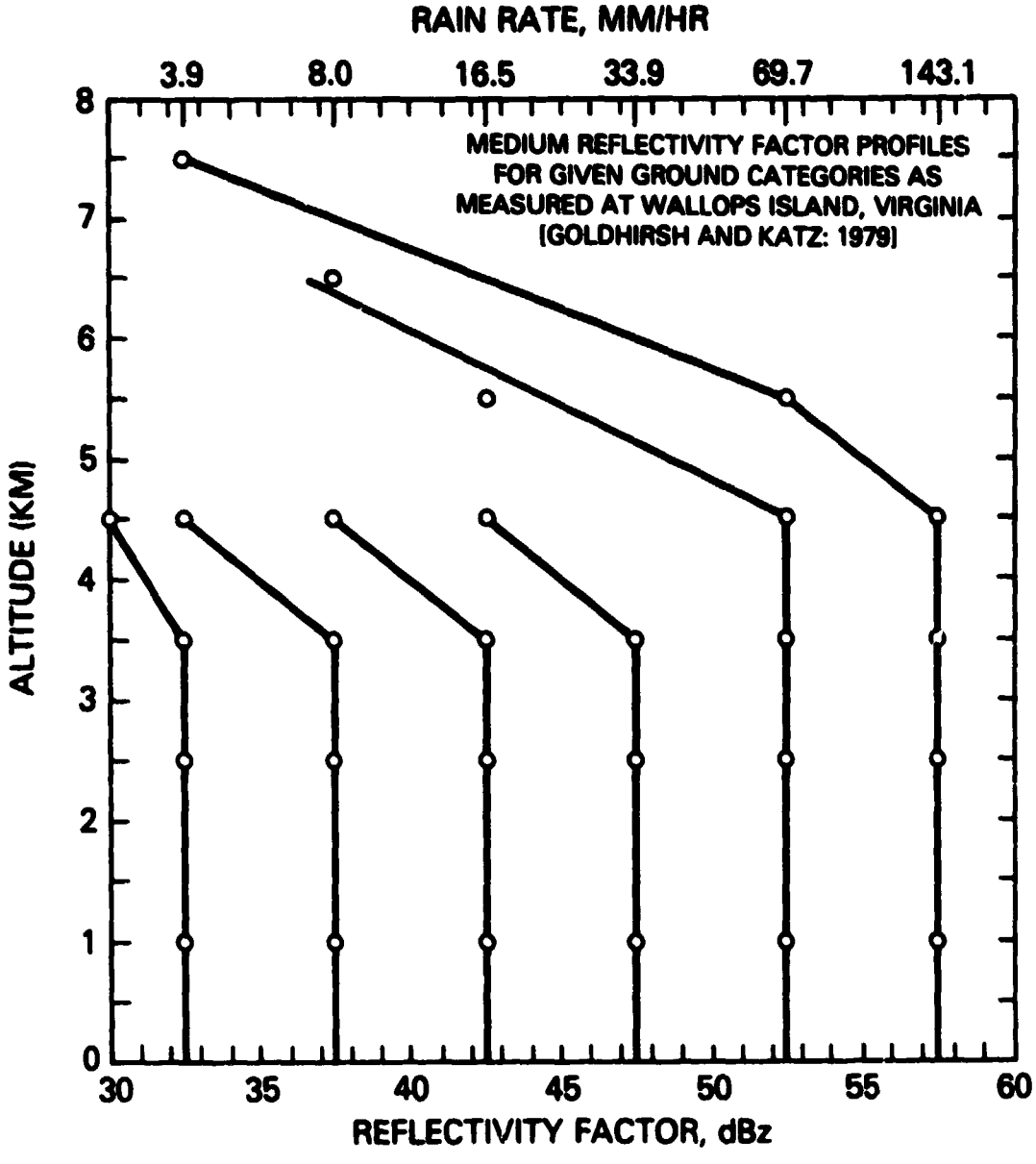

Figure 1. Measured reflectivity versus altitude for various rain rates.

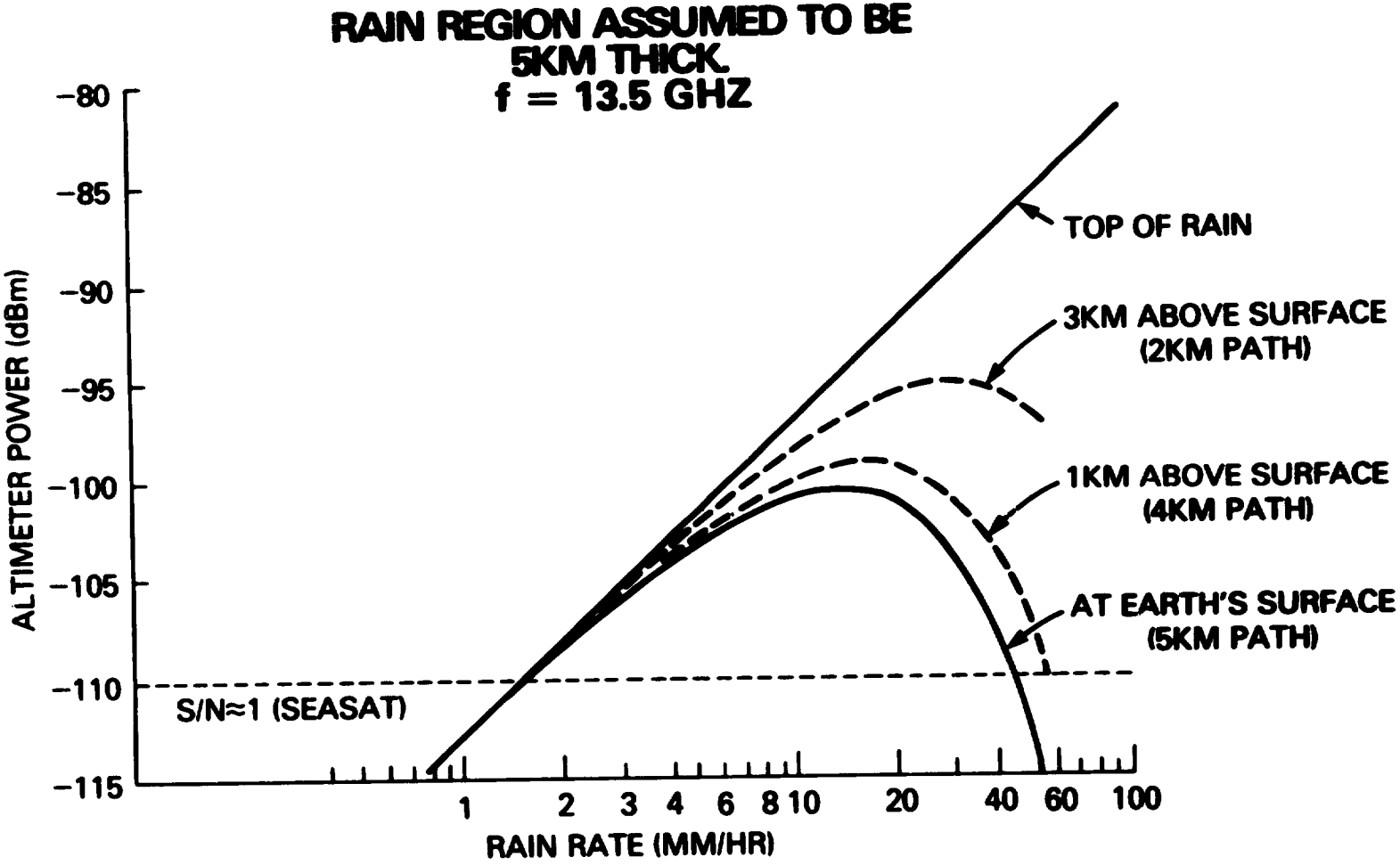

Figure 2. Reflectivities of Figure 1 translated into power received at the altimeter.

MODIFICATIONS TO SEASAT ALTIMETER ACQUISITION CIRCUITRY

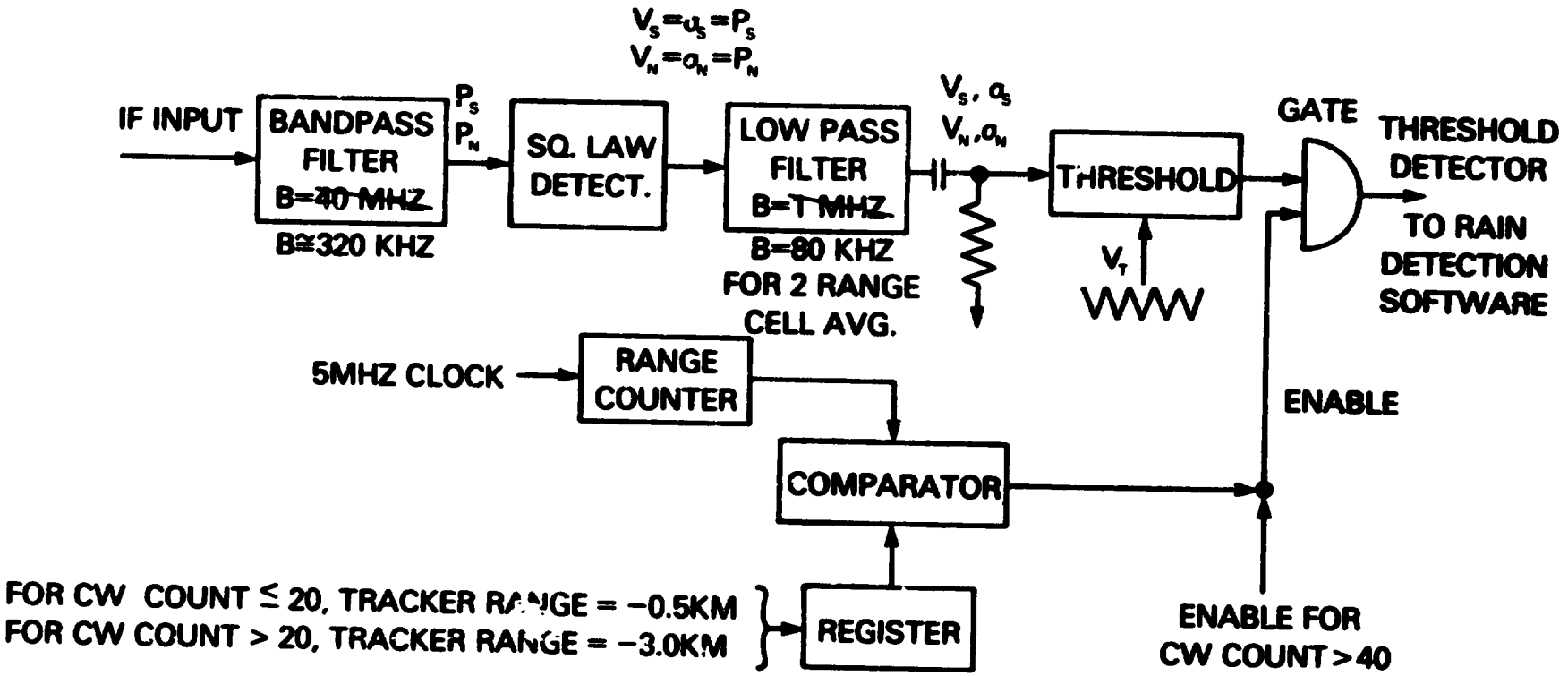

Figure 3. Hardware modifications to the altimeter acquisitions circuitry for the rain mode.

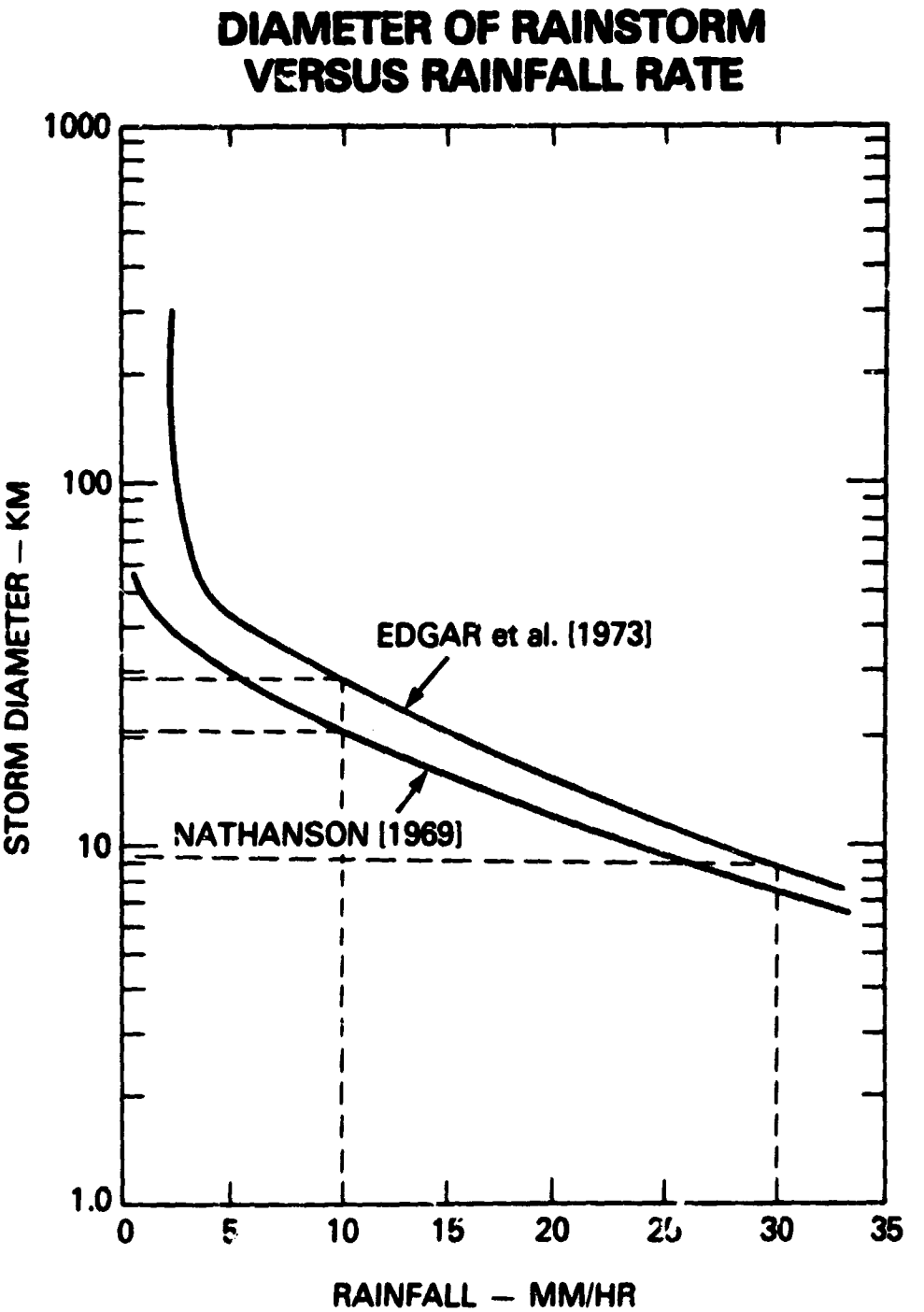

Figure 4. Typical diameters of rain storms as a function of rain rate.

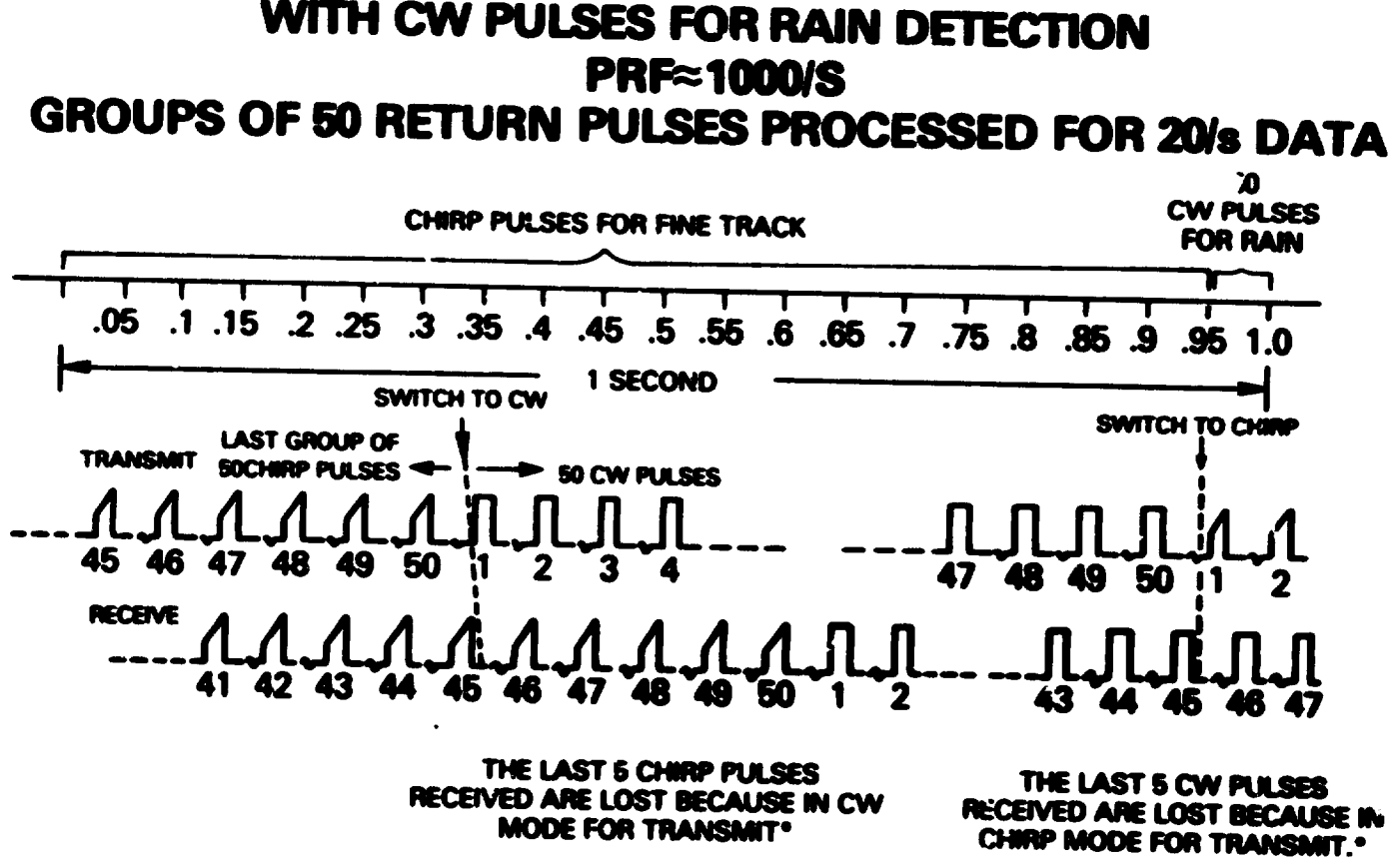

Figure 5. Arrangement of the transmitted and received pulses in the proposed rain detection implementation.

45 PULSES TO DETERMINE POWER AT 2 ALTITUDES AND ALTITUDE OF TOP OF RAIN

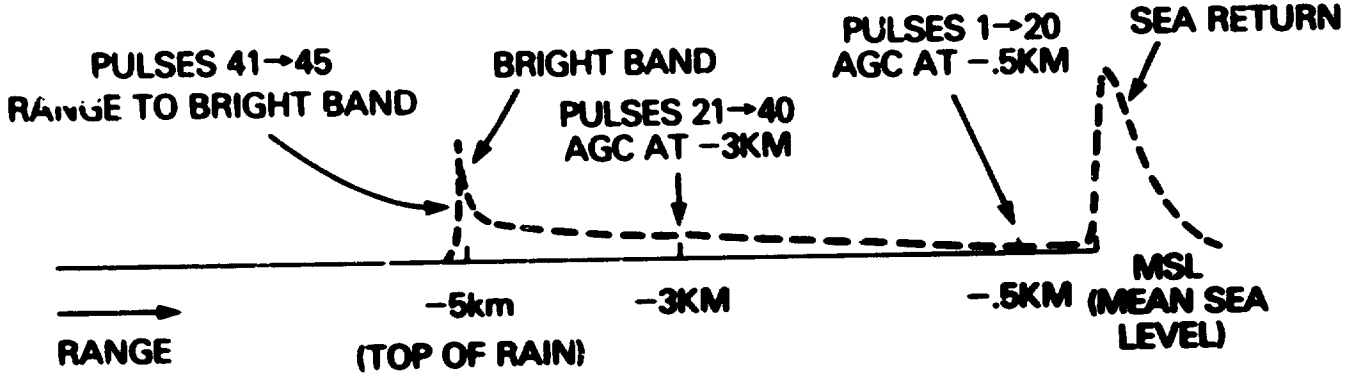

Figure 6. Utilization of pulses in rain mode.

AGC SETTLING

PULSES	AGC INCREMENT (dB)
1→4	2
5→11	1
> 11	0.25

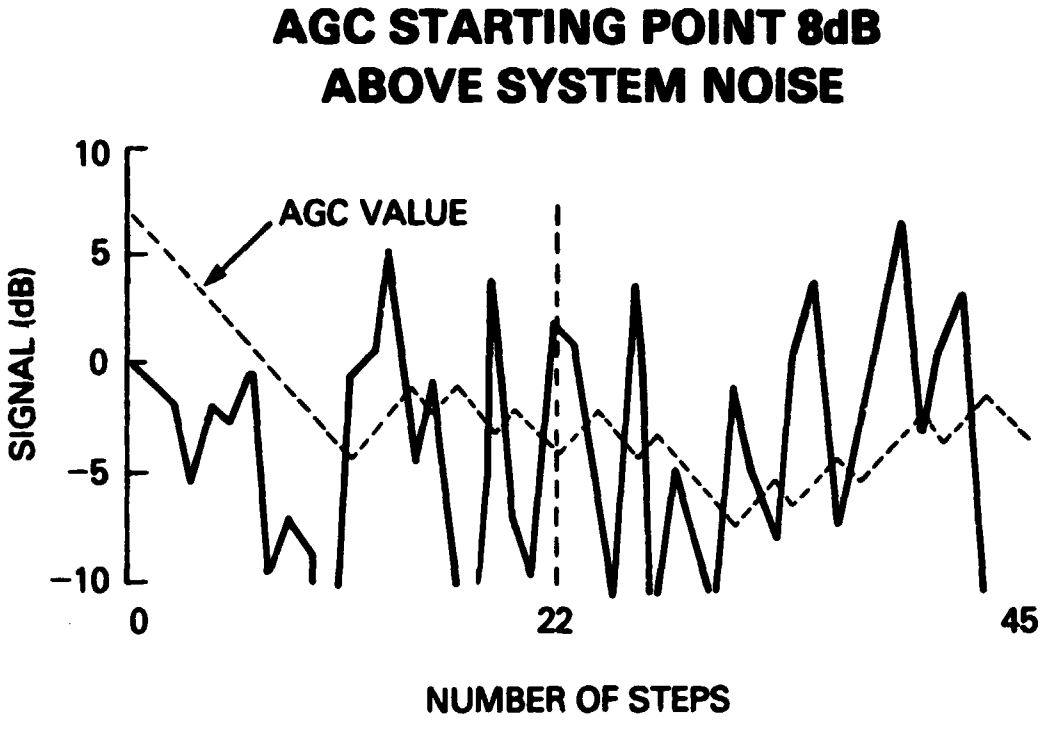

Figure 7. Results of simulation of the altimeter AGC settling over a series of 45 pulses.

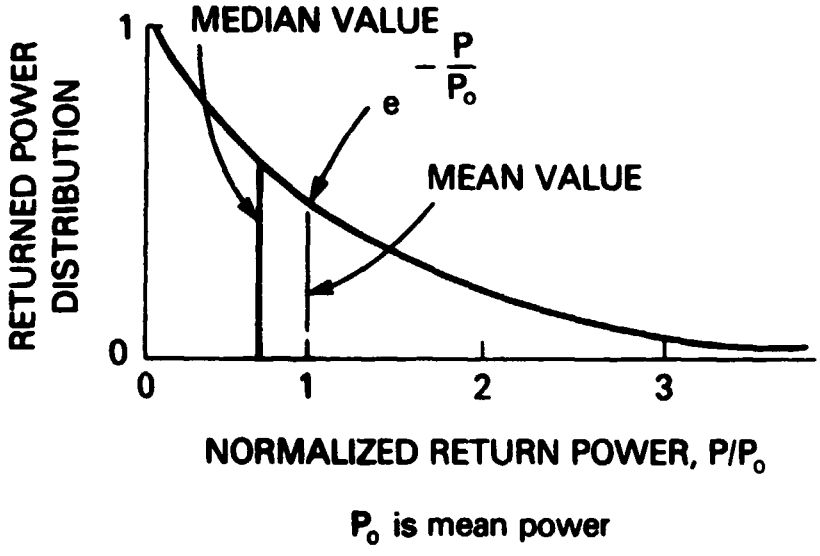

Figure 8. Returned power distribution indicating mean and median values.

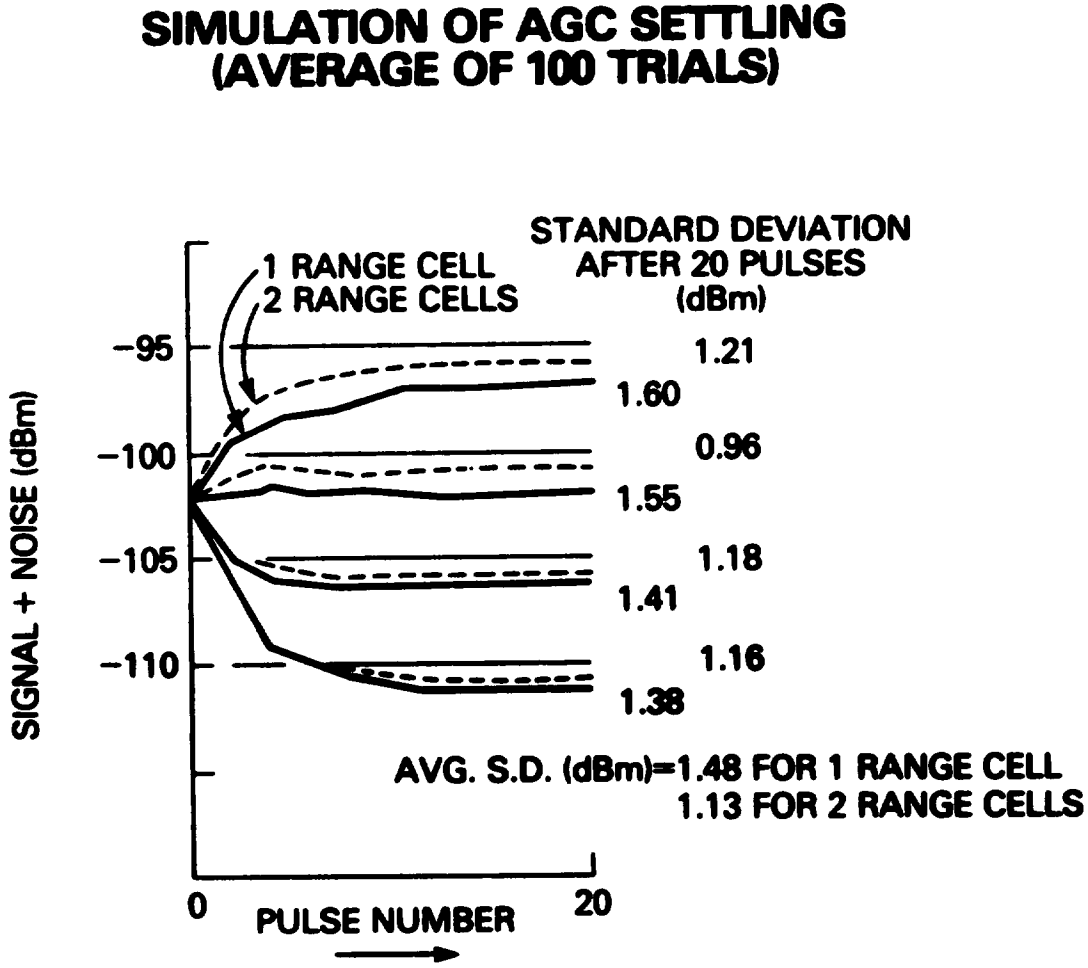

Figure 9. The manner in which altimeter AGC approaches the mean value for various values of signal plus noise.

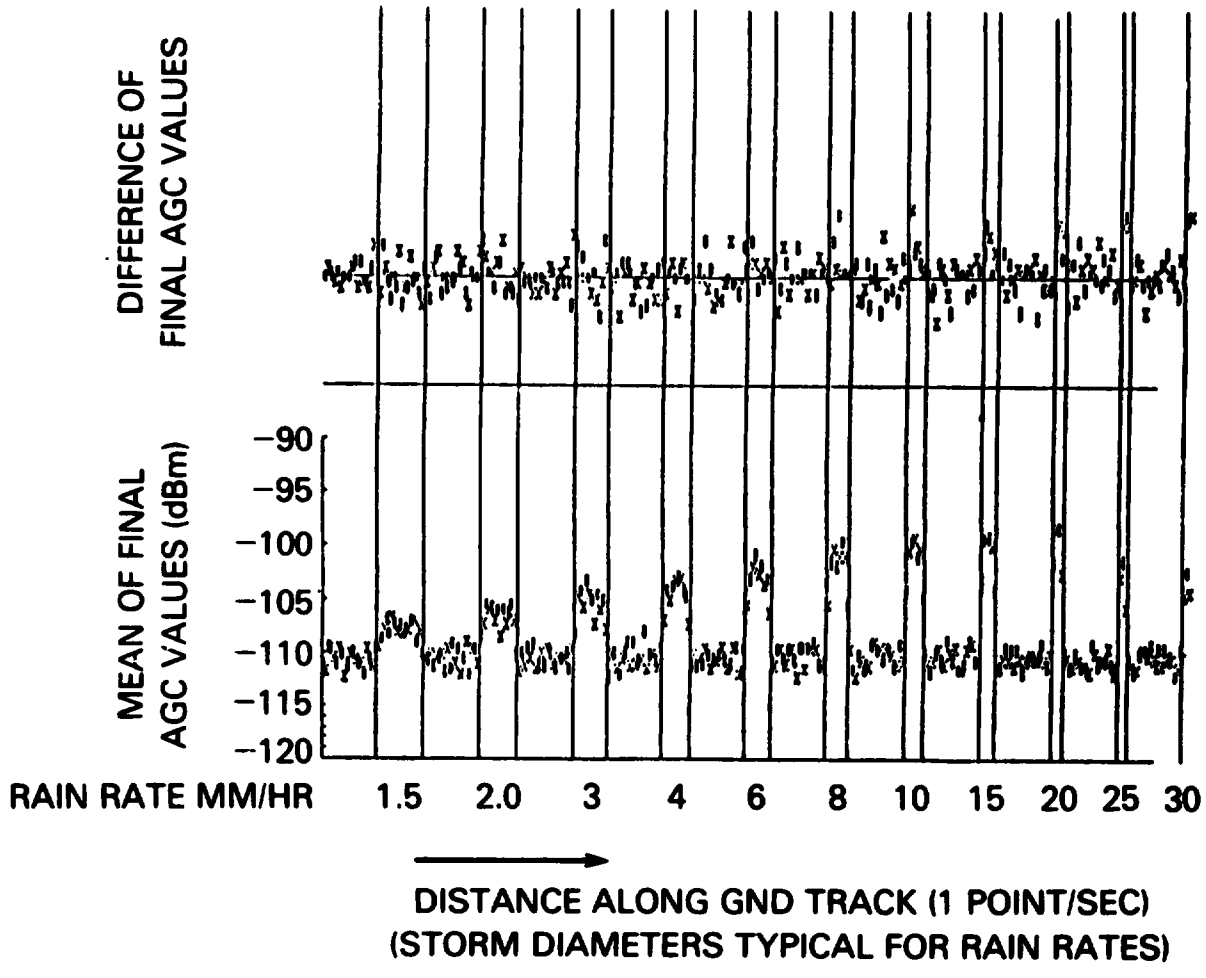

Figure 10. Simulation results for one altimeter pass where encountered periods for rains of various rates were determined by the average storm diameters of Figure 4.

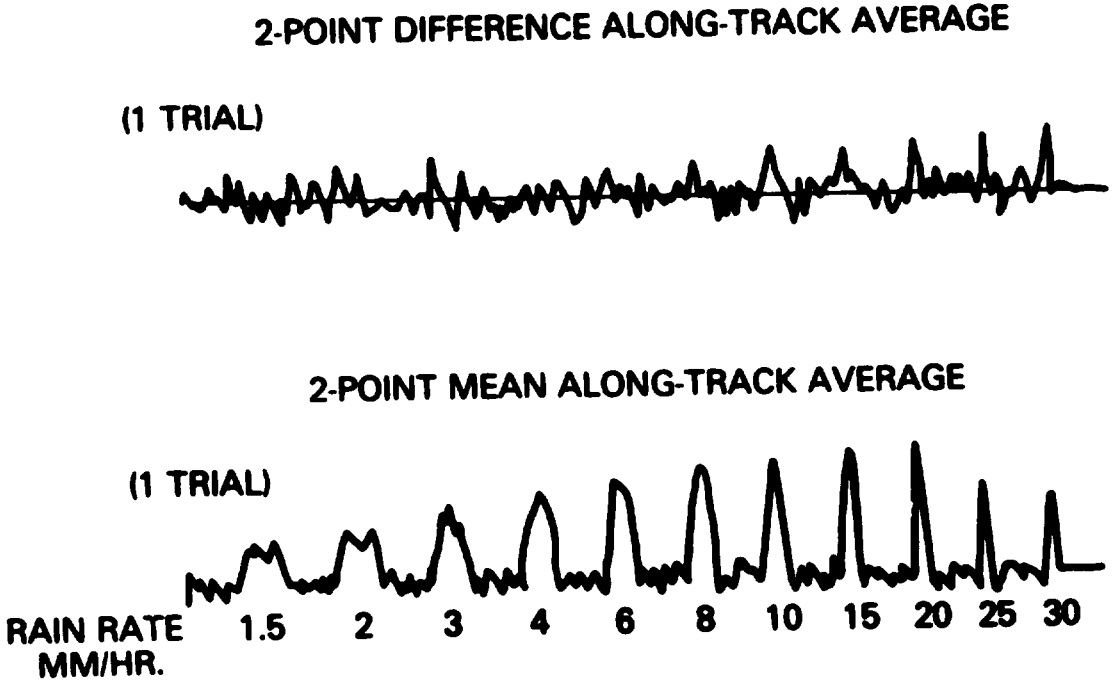

Figure 11. Data of Figure 10 after two-point along-track data averaging.